GEOLOGY | THE GEOLOGICAL SOCIETY OF AMERICA®

https://doi.org/10.1130/G50023.1

Manuscript received 11 January 2022
Revised manuscript received 11 April 2022
Manuscript accepted 17 April 2022

Published online 27 May 2022

Explosive-effusive-explosive: The role of magma ascent rates and paths in modulating caldera eruptions

Olivier Bernard[1,2], Weiran Li[3], Fidel Costa[1,2], Steve Saunders[4], Ima Itikarai[4], Mikhail Sindang[4] and Caroline Bouvet de Maisonneuve[1,2]

[1]Earth Observatory of Singapore, Nanyang Technological University, 50 Nanyang Avenue, Block N2-01a-15, Singapore 639798, Singapore
[2]Asian School of the Environment, Nanyang Technological University, 62 Nanyang Drive, Singapore 637459, Singapore
[3]Department of Earth Sciences, University of Cambridge, Downing Street, Cambridge CB2 3EQ, UK
[4]Rabaul Volcano Observatory, P.O. Box 386, Rabaul 611, Papua New Guinea

ABSTRACT

One of the biggest challenges in volcanology is assessing the role of magma properties (volatile budgets, storage depths, and ascent rates) in controlling eruption explosivity. We use a new approach based on apatite to estimate volatile contents and magma ascent rates from a sequence of sub-Plinian, effusive, and Vulcanian eruption deposits at Rabaul caldera (Papua New Guinea) emplaced in 2006 CE to probe the mechanisms responsible for the sudden transitions in eruption styles. Our findings show that all magmas were originally stored at similar conditions (2–4 km depth and 1.8–2.5 wt% H_2O in the melt); only the magma that formed the lava flow stalled and degassed at a shallower level (0.2–1.5 km) for several months. A more energetic batch of magma rose from depth, bypassed the transient reservoir, and ascended within ≤8 h to Earth's surface (mean velocity ≥0.2 m/s), yielding the initial sub-Plinian phase of the eruption. The shallowly degassed magma was then able to reach the surface as a lava flow, likely through the path opened by the sub-Plinian magma. The magma of the last Vulcanian phase ascended without storage at a shallow depth, albeit more slowly (ascent rate 0.03–0.1 m/s) than the sub-Plinian magma. Our study illustrates how the complexity of plumbing systems may affect eruption styles, including at other volcanic systems, and have implications for interpreting volcano monitoring data.

INTRODUCTION

Magma storage depth, pre-eruptive volatile budgets, and magma ascent rates are known to be controls on eruption explosivity (Burgisser and Degruyter, 2015). These three parameters can be interdependent; for example, the abundance of volatiles dissolved in the melt determines the pressure and extent of volatile exsolution during magma ascent, which influence magma buoyancy and ascent rate (Gonnermann and Manga, 2012). Estimating the three parameters is challenging because none of them is measurable and they are typically calculated by combining geophysical, petrological, and/or geochemical methods (e.g., Endo and Murray, 1991; Rutherford, 2008; Armienti et al., 2013) that mostly require lengthy analyses and several corrections and/or assumptions (Edmonds et al., 2019). Thus, it is desirable to find additional tools that can constrain all the above-mentioned parameters.

Magma volatile contents and storage depths are traditionally studied via melt-inclusion analysis. Recently the volatile-bearing mineral apatite has been found to be a good proxy not only for melt volatile budgets (Scott et al., 2015; Stock et al., 2018; Li and Costa, 2020) but also for magma ascent rates (when combined with zoning-pattern analysis; Li et al., 2020a, 2020b). We investigated the volatile chemistry of apatite from the 2006 CE eruption at Rabaul (Papua New Guinea; 4.2004°S, 152.163°E). This eruption was one of the most explosive events in a 20-year-long episode starting from 1994 (Global Volcanism Program, 2006) and had three phases: (1) a sub-Plinian onset that lasted for 12 hr, (2) an ~12 h mixed Strombolian-effusive phase, and (3) discrete Vulcanian explosions over two weeks. The eruption sequence was well documented by scientists at the Rabaul Volcano Observatory (RVO) and has been studied to reconstruct the volcano plumbing system and pre-eruptive magmatic processes (Bouvet de Maisonneuve et al., 2015). The presence of a large dacitic reservoir located at 3–6 km depth with magmas at ~950–1000 °C, which is frequently recharged with basaltic magmas (Itikarai, 2008; Johnson et al., 2010; Patia et al., 2017), was proposed. The minor compositional differences between products from the three phases led Bernard and Bouvet de Maisonneuve (2020) to propose that slight differences in the initial phenocryst abundances and melt water contents in the reservoir are responsible for the change in eruption styles. We investigated the cause of the eruption dynamics by quantifying magma storage conditions, time scales, and ascent rates using apatite.

METHODS

We studied samples that are representative of the sub-Plinian, effusive, and Vulcanian phases of the 2006 eruption: pumices in a tephra fall deposit, fragments of a lava flow, and fragments of a ballistic cowpie bomb (see a description in Bernard and Bouvet de Maisonneuve, 2020). Major element and volatile (including Cl and F) concentrations in matrix- and clinopyroxene (Cpx)–hosted apatite crystals, melt inclusions, and matrix glass (this study; Bouvet de Maisonneuve et al., 2015) were determined by an electron probe microanalyzer (EPMA). In total, 218 single-point analyses (with 10 μm beam size) were acquired from 161 apatite crystals (40–64 crystals per rock sample), which appear as either inclusions in Cpx or matrix-hosted microphenocrysts (>30 μm in length). Concentrations of OH were calculated from apatite stoichiometry

CITATION: Bernard, O., et al., 2022, Explosive-effusive-explosive: The role of magma ascent rates and paths in modulating caldera eruptions: Geology, v. 50, p. 1013–1017, https://doi.org/10.1130/G50023.1

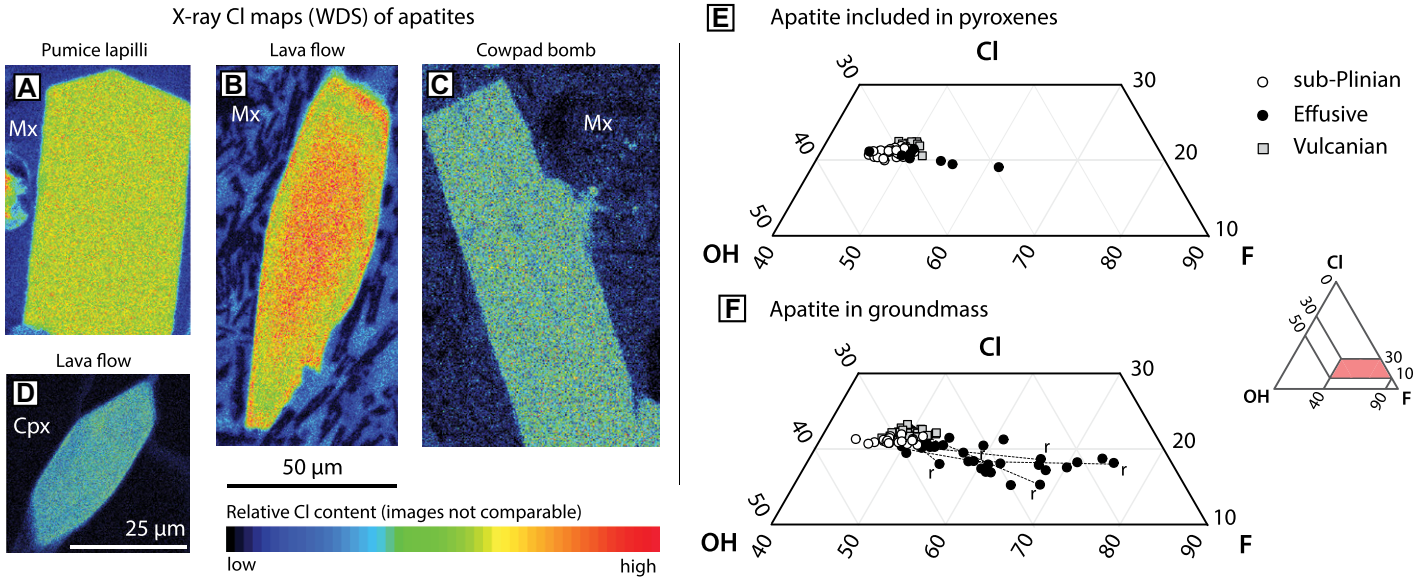

Figure 1. Apatite compositions of Rabaul caldera (Papua New Guinea) eruptive products. (A–D) Wavelength-dispersive spectrometry (WDS) X-ray maps of Cl (color scales vary between images) in matrix (Mx) apatite from each eruptive phase (A–C) and clinopyroxene (Cpx)–hosted apatite in lava (D). (E,F) F-Cl-OH compositions of Cpx-hosted apatite (E) and matrix apatite (F). Dotted lines link core and rim (labeled "r") point analyses acquired from same crystals in lava.

(see the Supplemental Material[1]). These results were used to calculate melt H_2O contents using the ApThermo model of Li and Costa (2020). Wavelength-dispersive spectrometry (WDS) X-ray maps of F and Cl (Figs. 1A–1D) and cathodoluminescence images were used to select zoned crystals for acquiring concentration profiles (1 µm beam size, nearly parallel to the crystal *c*-axes). We used the one-dimensional multicomponent (F-Cl-OH) diffusion model ApTimer (Li et al., 2020a) to fit the measured profiles ($n = 16$) and to estimate magma degassing time and ascent rates. Crystallographic orientations of apatite were accounted for in diffusion modeling (due to strong anisotropy of Cl diffusion; Li et al., 2020a), and root-mean-square deviation (RMSD) was used to assess the goodness of fit. Additional details on the samples and analytical methods are provided in the Supplemental Material.

RESULTS

Apatite Volatile Compositions and Melt Water Contents

Apatite crystals in Cpx from the pumice (sub-Plinian), bomb (Vulcanian), and lava flow (effusive) show a similar and narrow range of F-Cl-OH contents (Figs. 1E and 1F) but differ in zoning patterns. Matrix-hosted apatite in the lava shows decreasing OH and increasing F toward the rim of individual crystals (Fig. 1F). WDS X-ray maps show a decrease in Cl concentration from crystal core to rim, followed by a sharp and narrow increase at the rim, most visible parallel to the *c*-axis (Fig. 1B). The Cpx- and matrix-hosted apatite in the pumice and bomb are not zoned in F or Cl, based on X-ray maps (Figs. 1A and 1C). Concentration profiles in the bomb's matrix apatite show narrow (~3 µm wide) zonation at crystal rims, which was not observed in any crystals of the pumice.

The pre-eruptive melt H_2O contents calculated from apatite (Fig. 2) range from 1.3 (± 0.5) to 3.0 (± 1.1) wt%, except those from the lava's matrix apatite rims at 0.4 (± 0.2) wt%. These agree with measurements in plagioclase- and pyroxene-hosted melt inclusions and in matrix glass in the pumice (Bouvet de Maisonneuve et al., 2015). Except for the lava, the Cpx- and matrix-hosted apatite of the sub-Plinian and Vulcanian eruptions give similar melt H_2O contents, implying limited extent of water exsolution before the two events, in contrast to the effusive one.

Diffusion Time Scales

With evidence of roughly 10 × longer zoning distances of F-Cl than rare earth elements in our crystals (see details in the Supplemental Material), we considered diffusion (rather than growth) as the main contributor to the observed F-Cl zoning. Rimward F-Cl-OH profiles of the lava and bomb matrix apatite were fit by diffusion modeling to estimate time scales that can be linked to magma degassing during ascent (Fig. 3). The Cl profiles of matrix apatite (Fig. 3) show a "trough" ~3–10 µm away from the crystal rim, which can be explained by the complex coupled diffusion of F-Cl-OH (Li et al., 2020a). Using constant boundary conditions in our model, we obtained well-fitted Cl profiles for apatite from the bomb but poorer fits for the lava apatite. This potentially implies varying boundary concentrations with time during

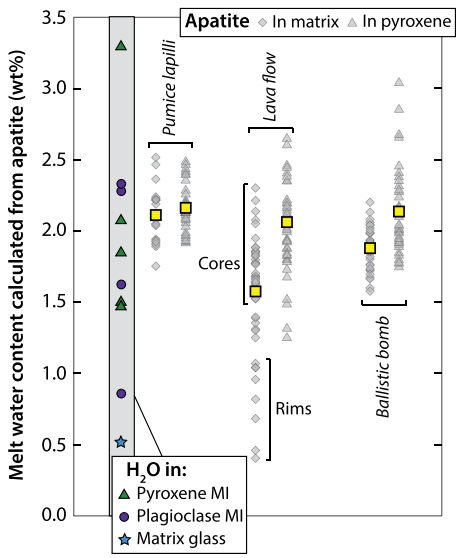

Figure 2. Melt H_2O contents for Rabaul caldera (Papua New Guinea) eruptive products (gray symbols; mean as yellow squares) calculated using the apatite-melt hygrometer of Li and Costa (2020). Data in the gray band are direct secondary ion mass spectrometry (SIMS) measurements of H_2O in glass and melt inclusions (MI) reported by Bouvet de Maisonneuve et al. (2015).

[1]Supplemental Material. Details on the methods and all fitted diffusion profiles, and a dataset containing the apatite single points and traverses data, water content values, and diffusion modelling parameters. Please visit https://doi.org/10.1130/GEOL.S.19783093 to access the supplemental material, and contact editing@geosociety.org with any questions.

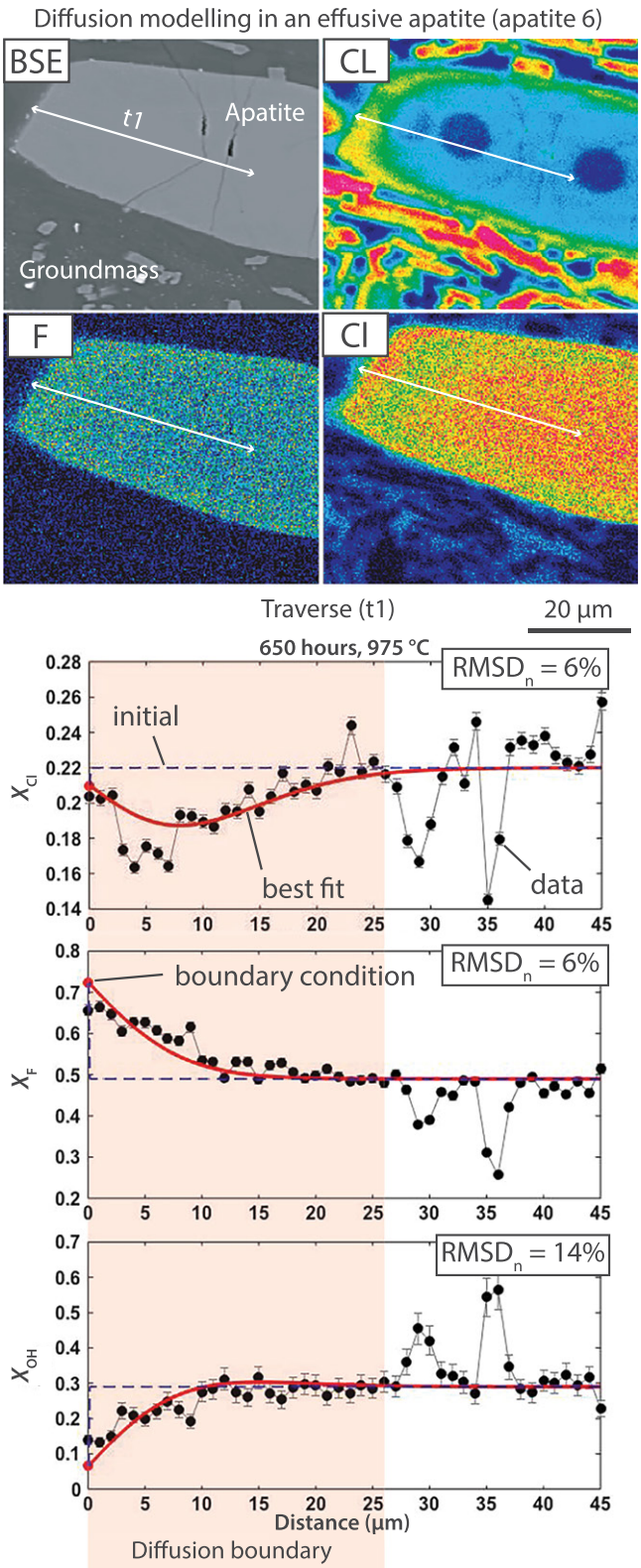

Figure 3. Example of model fits for Cl-F-OH diffusion in apatite from Rabaul caldera (Papua New Guinea) lava flow. BSE—backscattered electron image, CL—cathodoluminescence image; F, Cl—fluorine and chlorine wavelength-dispersive spectrometry (WDS) X-ray maps; RMSD$_n$—normalized root-mean-square deviation (see the Supplemental Material [see footnote 1]).

magma degassing and requires future modeling efforts. Using 975 °C (two-pyroxene thermometry), we obtain diffusion times of ~9–28 h for the bomb samples ($n = 6$) and much longer times for the lava samples (~650–2200 h ≈ 1–3 months; $n = 6$). The absence of zoning in the pumice apatite implies much shorter times: at maximum 8 h, assuming the zoning distance measurable from this study is 2 µm ($n = 4$). The main source of error in the time scales comes from the uncertainty in temperature (T; Fig. 4): decreasing T by 25 °C increases the time estimate by a factor of 1.5–2 (e.g., ~3–10 months at 925 °C for the lava).

DISCUSSION

Volatile Saturation and Magma Storage Pressure

Water solubility in silicate melts is mostly controlled by pressure and melt composition (Newman and Lowenstern, 2002); the latter plays a negligible role in this study because all deposits have similar bulk-rock and glass compositions (Bernard and Bouvet de Maisonneuve, 2020). Using the average H_2O contents calculated from Cpx-hosted apatite core compositions for the three eruptive phases, we can estimate volatile saturation pressures using the H_2O-CO_2 solubility model of Papale et al. (2006). At 975 °C and assuming no CO_2 in the melt, we obtained H_2O saturation pressures of 30–60 MPa for all three deposits. The addition of ~150 ppm CO_2 in the melt (the mean of CO_2 in pumice Cpx-hosted melt inclusions; Bouvet de Maisonneuve et al., 2015) increases volatile saturation pressures to 50–100 MPa, corresponding to 2–4 km below the crater (taking a mean crustal density of 2600 kg/m^3). These agree with the 3–6 km depth of the main reservoir at Rabaul derived from geophysical and other petrological tools (Saunders, 2001; Itikarai, 2008; Bouvet de Maisonneuve et al., 2015). Melt H_2O contents derived from the lava's matrix apatite rims (0.4 ± 0.2 to 1.4 ± 0.5 wt% H_2O; Fig. 2) give us H_2O saturation pressures that translate to magma storage depths of 0.2–1.5 km. These are much shallower than those of the more explosive phases but are still beneath the surface. This implies that the magma that fed the lava flow resided in a storage zone close to the surface where the melt degassed and that such storage did not happen before the more explosive phases.

Relative Timing of Reservoir and Conduit Processes during the 2006 Eruption

The magma storage depth and time scales of degassing and residence we reported above provide insights for better interpreting the monitoring data of Rabaul caldera, which is continuously monitored by RVO (McKee et al., 2018). Prior to the 2006 eruption, an uplift of ~15 cm was recorded in January–September 2005 and February–October 2006 (GPS time series in Fig. 4). Such deformation was likely related to mafic magma replenishment up to 10 days prior to the eruption (Fig. 4; Bouvet de Maisonneuve et al. 2015). On a shorter time scale, a threefold increase in the real-time seismic amplitude measurement (RSAM; Fig. 4) started 8 h before the sub-Plinian onset of the eruption and likely reflects fast magma movement to the surface. The time scale is in accord with our time estimates (<8 h) from the unzoned pumice apatite (Fig. 4B).

Following the initial explosive sub-Plinian phase, a lava flow was erupted from the same vent (similarly to Cordón Caulle, Chile; Castro et al., 2013) in a span of a few hours (Global Volcanism Program, 2006). From

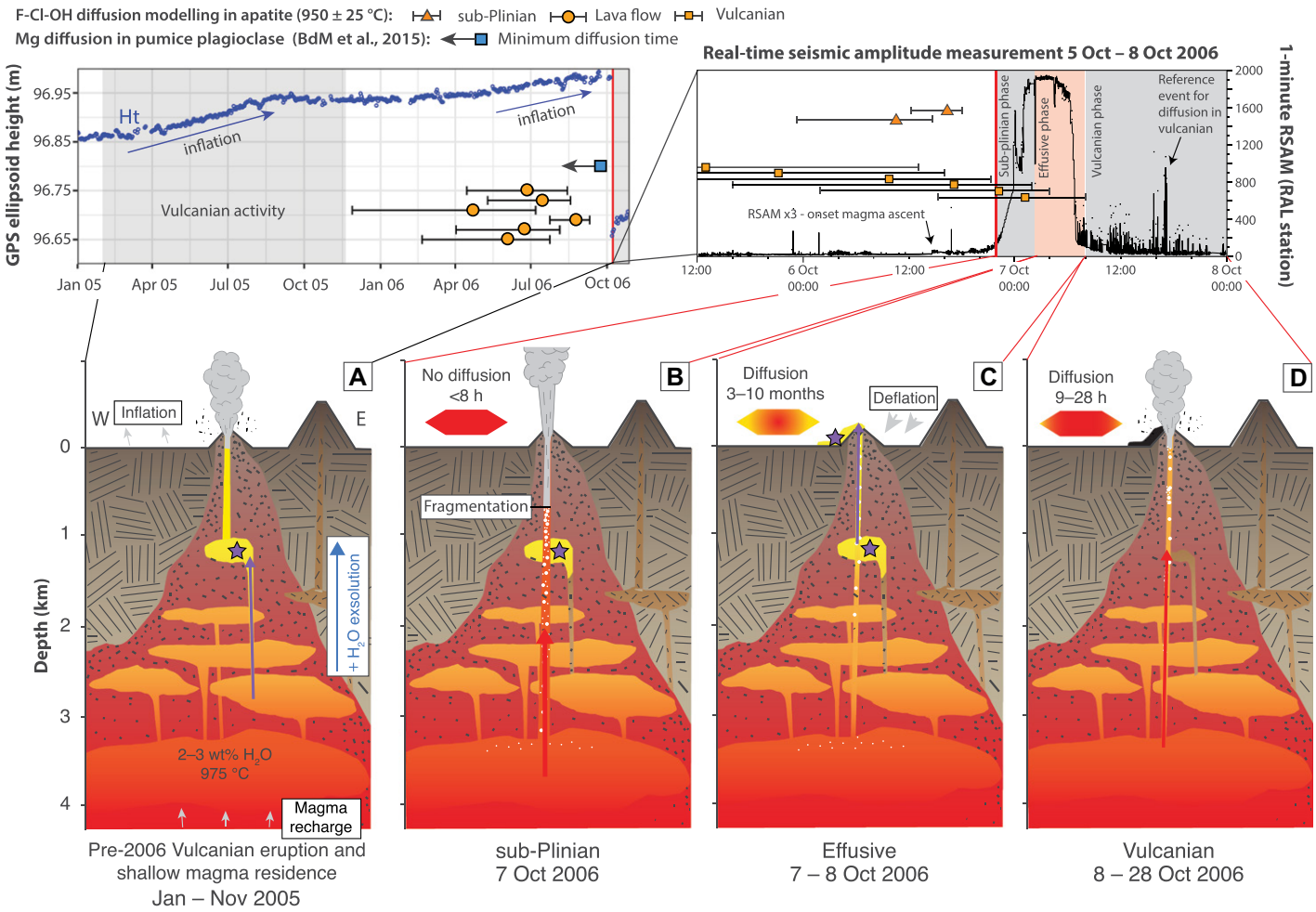

Figure 4. Proposed model for reservoir and conduit processes during the 2006 eruption of Rabaul caldera (Papua New Guinea) in relation to monitoring and petrological data. Top left: F-Cl-OH diffusion times of lava apatite (orange circles) and real-time GPS measurements (ellipsoid height, Ht). BdM et al., 2015—Bouvet de Maisonneuve et al. (2015). Top right: Real-time seismic amplitude measurement (RSAM) time series from 5–8 October 2006 (Greenwich Mean Time) in relation to Vulcanian and sub-Plinian apatite (orange squares and triangles, respectively). Error bars reflect uncertainties in diffusion times using a temperature of 950 ± 25 °C. Eruption onset is marked by the vertical red line. Panels A–D at bottom illustrate the evolution of Rabaul's plumbing system from 2005 throughout the 2006 eruption. They are arranged in time order (starting with leftmost), where purple arrows and stars indicate the locations of effusive magma and red to yellow polygons illustrate diffusion processes in apatite through the eruption.

matrix-hosted apatite, we found evidence of melt water degassing for 1–10 months prior to eruption at 0.2–1.5 km depth (Fig. 4). Given the deeper original depth found for this magma (2–4 km, according to Cpx-hosted apatite), this timing implies that the effusively erupted magma started ascending much earlier than the sub-Plinian magma batch. The spatial resolution of our estimates does not allow discrimination between a slow, multi-step ascent versus a single-step ascent to intermediate depths. Nevertheless, magma movement and storage at these depths for several months allowed further degassing and crystallization, which eventually resulted in an effusive eruption. The longest degassing time of ~10 months suggests magma ascent could have started by the end of the first uplift period between January and November 2005, when Vulcanian activity and ash venting occurred (Fig. 4A). The subsequent rise of the volatile-rich and buoyant sub-Plinian magma batch bypassed this more degassed magma and may have opened and/or widened the pathway, allowing the effusive magma batch to ascend more easily (Fig. 4C; e.g., Thomas and Neuberg, 2014).

Following the effusive phase, Vulcanian eruptions occurred with decreasing frequency over two weeks (Fig. 4D). The melt H_2O contents calculated from Cpx-hosted apatite in the bomb indicate similar depths of pre-eruptive storage as those of magmas of the other eruption phases. Instead of stalling at 0.2–1.5 km depth, this magma was able to ascend to the ground surface within a day, likely because the system had become more open after the ascent of the sub-Plinian and effusive magmas.

Magma Ascent Rates and Implications for Eruption Explosivity

Using 3–6 km as the reservoir depth and ≤8 h of ascent time for the sub-Plinian magma batch, we estimate a minimum ascent rate of 0.1–0.2 m/s. Bernard and Bouvet de Maisonneuve (2020) found an ascent rate two orders of magnitude higher of ~40 m/s using permeability and clast sizes (Rust and Cashman, 2011). The two estimates are not inconsistent because the latter one was calculated at the fragmentation depth where ascent velocity is the greatest whereas the diffusion model yields a maximum time (given no zoning in the sub-Plinian apatite) and thus a minimum ascent rate. For the Vulcanian phase, the 9–28 h of magma ascent translate into an average velocity of 0.03–0.1 m/s, in agreement with that of 0.1 m/s found by Bernard and Bouvet de Maisonneuve (2020) from microlites. The drop of ascent rate from the sub-Plinian to the Vulcanian magma batch, despite their similar pre-eruptive melt volatile contents, could be explained by a drop in overpressure in the system after the sub-Plinian event (intense deflation shown by GPS data; Fig. 4), with pos-

sibly significant changes in the system configuration such as partial collapse and/or closure of the conduit (de' Michieli Vitturi et al., 2010; Aravena et al., 2018). For the effusive phase, the long zoning distances in apatite include those of the final, decompression-related zoning caused by magma degassing from intermediate depths to the surface. The difference in ascent rates of the eruption phases, resulting in drastic changes in eruption dynamics, can be attributed to a combination of (1) different depths of pre-eruptive residence, which allowed parental magmas to lose volatiles at different rates (sub-Plinian and Vulcanian versus effusive), and (2) a drop in mass eruption rate due to decrease in overpressure (sub-Plinian versus Vulcanian). This is fundamental for interpreting monitoring data at calderas in terms of pre-eruptive magma transfer, especially in the case of extended periods of unrest.

CONCLUSIONS

We have shown that the eruption sequence of Rabaul caldera at the surface, from explosive (sub-Plinian) to effusive (lava) and back to explosive (Vulcanian), is distinct from, and thus does not reflect, the sequence of magma movement at depth. We show evidence of an early ascent and stalling at intermediate depth of the magma that led to the effusive lava eruption; this was followed several months later by the ascent of the sub-Plinian and Vulcanian magma batches. Our finding has important implications for interpretation of monitoring data in terms of subsurface magma-transfer dynamics. Lava effusion following the sub-Plinian eruption was the result of several months of magma storage and degassing, the timing of which is consistent with deformation changes, potentially suggesting a connection to mafic magma recharging the system during that period. The fast ascent of the sub-Plinian magma (within a few hours) agrees with the abrupt escalation of real-time seismic amplitude measurement data. Our study also shows that using commonly accessible instruments (scanning electron microscopy and EPMA) combined with thermodynamic and diffusion modeling of apatite, we can obtain volatile contents and degassing time scales of magmas, which are very difficult to acquire simultaneously otherwise.

ACKNOWLEDGMENTS

We thank M. Streck and M. Cassidy for insightful reviews, and M. Norman for editorial handling. This work was supported by the National Research Foundation (NRF) Singapore and the Singapore Ministry of Education under the Research Centres of Excellence initiative, as well as the NRF grant NRF-NRFF2016-04. This is EOS contribution number 440.

REFERENCES CITED

Aravena, Á., Cioni, R., de'Michieli Vitturi, M., and Neri, A., 2018, Conduit stability effects on intensity and steadiness of explosive eruptions: Scientific Reports, v. 8, 4125, https://doi.org/10.1038/s41598-018-22539-8.

Armienti, P., Perinelli, C., and Putirka, K.D., 2013, A new model to estimate deep-level magma ascent rates, with applications to Mt. Etna (Sicily, Italy): Journal of Petrology, v. 54, p. 795–813, https://doi.org/10.1093/petrology/egs085.

Bernard, O., and Bouvet de Maisonneuve, C., 2020, Controls on eruption style at Rabaul, Papua New Guinea—Insights from microlites, porosity and permeability measurements: Journal of Volcanology and Geothermal Research, v. 406, 107068, https://doi.org/10.1016/j.jvolgeores.2020.107068.

Bouvet de Maisonneuve, C., Costa, F., Patia, H., and Huber, C., 2015, Mafic magma replenishment, unrest, and eruption in a caldera setting: Insights from the 2006 eruption of Rabaul (Papua New Guinea), *in* Caricchi, L., and Blundy, J.D., eds., Chemical, Physical and Temporal Evolution of Magmatic Systems: Geological Society, London, Special Publication 422, p. 17–39, https://doi.org/10.1144/SP422.2.

Burgisser, A., and Degruyter, W., 2015, Magma ascent and degassing at shallow levels, *in* Sigurdsson, H., ed., The Encyclopedia of Volcanoes (second edition): Amsterdam, Academic Press, p. 225–236, https://doi.org/10.1016/B978-0-12-385938-9.00011-0.

Castro, J.M., Schipper, C.I., Mueller, S.P., Militzer, A.S., Amigo, A., Parejas, C.S., and Jacob, D., 2013, Storage and eruption of near-liquidus rhyolite magma at Cordón Caulle, Chile: Bulletin of Volcanology, v. 75, p. 702, https://doi.org/10.1007/s00445-013-0702-9.

de' Michieli Vitturi, M., Clarke, A.B., Neri, A., and Voight, B., 2010, Transient effects of magma ascent dynamics along a geometrically variable dome-feeding conduit: Earth and Planetary Science Letters, v. 295, p. 541–553, https://doi.org/10.1016/j.epsl.2010.04.029.

Edmonds, M., Cashman, K.V., Holness, M., and Jackson, M., 2019, Architecture and dynamics of magma reservoirs: Philosophical Transactions of the Royal Society A: Mathematical, Physical, and Engineering Sciences, v. 377, 20180298, https://doi.org/10.1098/rsta.2018.0298.

Endo, E.T., and Murray, T., 1991, Real-time Seismic Amplitude Measurement (RSAM): A volcano monitoring and prediction tool: Bulletin of Volcanology, v. 53, p. 533–545, https://doi.org/10.1007/BF00298154.

Global Volcanism Program, 2006, Report on Rabaul (Papua New Guinea): Bulletin of the Global Volcanism Network, v. 31, no. 9, https://doi.org/10.5479/si.GVP.BGVN200609-252140.

Gonnermann, H.M., and Manga, M., 2012, Dynamics of magma ascent in the volcanic conduit, *in* Fagents, S.A., et al., eds., Modeling Volcanic Processes: The Physics and Mathematics of Volcanism: Cambridge, UK, Cambridge University Press, p. 55–84, https://doi.org/10.1017/CBO9781139021562.004.

Itikarai, I., 2008, The 3-D structure and earthquake locations at Rabaul Caldera, Papua New Guinea [M.Phil. thesis]: Canberra, Australian National University, 193 p., https://doi.org/10.25911/5d5156d4a7f51.

Johnson, R.W., Itikarai, I., Patia, H., and McKee, C.O., 2010, Volcanic systems of the northeastern Gazelle Peninsula, Papua New Guinea: Synopsis, evaluation, and a model for Rabaul Volcano: Port Moresby, Papua New Guinea, Rabaul Observatory Twinning Program, Papua New Guinea Department of Mineral Policy and Geohazards Management and Australian Agency for International Development, 84 p.

Li, W., and Costa, F., 2020, A thermodynamic model for F-Cl-OH partitioning between silicate melts and apatite including non-ideal mixing with application to constraining melt volatile budgets: Geochimica et Cosmochimica Acta, v. 269, p. 203–222, https://doi.org/10.1016/j.gca.2019.10.035.

Li, W., Chakraborty, S., Nagashima, K., and Costa, F., 2020a, Multicomponent diffusion of F, Cl and OH in apatite with application to magma ascent rates: Earth and Planetary Science Letters, v. 550, 116545, https://doi.org/10.1016/j.epsl.2020.116545.

Li, W., Costa, F., and Nagashima, K., 2020b, Apatite crystals reveal melt volatile budgets and magma storage depths at Merapi volcano, Indonesia: Journal of Petrology, v. 62, egaa100, https://doi.org/10.1093/petrology/egaa100.

McKee, C., Itikarai, I., and Davies, H., 2018, Instrumental volcano surveillance and community awareness in the lead-up to the 1994 eruptions at Rabaul, Papua New Guinea, *in* Fearnley, C.J., et al., eds., Observing the Volcano World: Volcano Crisis Communication: Cham, Springer International Publishing, p. 205–233, https://doi.org/10.1007/11157_2017_4.

Newman, S., and Lowenstern, J.B., 2002, VolatileCalc: A silicate melt-H_2O-CO_2 solution model written in Visual Basic for Excel: Computers & Geosciences, v. 28, p. 597–604, https://doi.org/10.1016/S0098-3004(01)00081-4.

Papale, P., Moretti, R., and Barbato, D., 2006, The compositional dependence of the saturation surface of $H_2O + CO_2$ fluids in silicate melts: Chemical Geology, v. 229, p. 78–95, https://doi.org/10.1016/j.chemgeo.2006.01.013.

Patia, H., Eggins, S.M., Arculus, R.J., McKee, C.O., Johnson, R.W., and Bradney, A., 2017, The 1994–2001 eruptive period at Rabaul, Papua New Guinea: Petrological and geochemical evidence for basalt injections into a shallow dacite magma reservoir, and significant SO_2 flux: Journal of Volcanology and Geothermal Research, v. 345, p. 200–217, https://doi.org/10.1016/j.jvolgeores.2017.08.011.

Rust, A.C., and Cashman, K.V., 2011, Permeability controls on expansion and size distributions of pyroclasts: Journal of Geophysical Research, v. 116, B11202, https://doi.org/10.1029/2011JB008494.

Rutherford, M.J., 2008, Magma ascent rates: Reviews in Mineralogy and Geochemistry, v. 69, p. 241–271, https://doi.org/10.2138/rmg.2008.69.7.

Saunders, S.J., 2001, The shallow plumbing system of Rabaul caldera: A partially intruded ring fault?: Bulletin of Volcanology, v. 63, p. 406–420, https://doi.org/10.1007/s004450100159.

Scott, J.A.J., Humphreys, M.C.S., Mather, T.A., Pyle, D.M., and Stock, M.J., 2015, Insights into the behaviour of S, F, and Cl at Santiaguito Volcano, Guatemala, from apatite and glass: Lithos, v. 232, p. 375–394, https://doi.org/10.1016/j.lithos.2015.07.004.

Stock, M.J., Humphreys, M.C.S., Smith, V.C., Isaia, R., Brooker, R.A., and Pyle, D.M., 2018, Tracking volatile behaviour in sub-volcanic plumbing systems using apatite and glass: Insights into pre-eruptive processes at Campi Flegrei, Italy: Journal of Petrology, v. 59, p. 2463–2492, https://doi.org/10.1093/petrology/egy020.

Thomas, M.E., and Neuberg, J.W., 2014, Understanding which parameters control shallow ascent of silicic effusive magma: Geochemistry Geophysics Geosystems, v. 15, p. 4481–4506, https://doi.org/10.1002/2014GC005529.

Printed in USA